

See discussions, stats, and author profiles for this publication at: <https://www.researchgate.net/publication/270706140>

Square–Antiprismatic Eight–Coordinate Complexes of Divalent First–Row Transition Metal Cations: A Density Functional Theory Exploration of the Electronic–Structural Landscape

ARTICLE *in* INORGANIC CHEMISTRY · JANUARY 2015

Impact Factor: 4.76 · DOI: 10.1021/ic502287m · Source: PubMed

CITATION

1

READS

19

4 AUTHORS, INCLUDING:



Jeanet Conradie

University of the Free State

142 PUBLICATIONS 1,856 CITATIONS

SEE PROFILE



Todd C Harrop

University of Georgia

39 PUBLICATIONS 775 CITATIONS

SEE PROFILE



Abhik Ghosh

UiT - The Arctic University of Norway

187 PUBLICATIONS 5,406 CITATIONS

SEE PROFILE

Square-Antiprismatic Eight-Coordinate Complexes of Divalent First-Row Transition Metal Cations: A Density Functional Theory Exploration of the Electronic–Structural Landscape

Janet Conradie,^{†,‡} Ashis K. Patra,[§] Todd C. Harrop,[§] and Abhik Ghosh^{*,†}

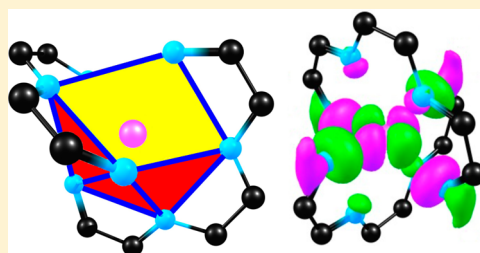
[†]Department of Chemistry and Center for Theoretical and Computational Chemistry, University of Tromsø, 9037 Tromsø, Norway

[‡]Department of Chemistry, University of the Free State, 9300 Bloemfontein, Republic of South Africa

[§]Department of Chemistry and Center for Metalloenzyme Studies, The University of Georgia, Athens, Georgia 30602, United States

Supporting Information

ABSTRACT: Density functional theory (in the form of the PW91, BP86, OLYP, and B3LYP exchange–correlation functionals) has been used to map out the low-energy states of a series of eight-coordinate square-antiprismatic (D_{2d}) first-row transition metal complexes, involving Mn(II), Fe(II), Co(II), Ni(II), and Cu(II), along with a pair of tetradentate N_4 ligands. Of the five complexes, the Mn(II) and Fe(II) complexes have been synthesized and characterized structurally and spectroscopically, whereas the other three are as yet unknown. Each N_4 ligand consists of a pair of terminal imidazole units linked by an *o*-phenylenediimine unit. The imidazole units are the strongest ligands in these complexes and dictate the spatial disposition of the metal three-dimensional orbitals. Thus, the $d_{x^2-y^2}$ orbital, whose lobes point directly at the coordinating imidazole nitrogens, has the highest orbital energy among the five d orbitals, whereas the d_{xy} orbital has the lowest orbital energy. In general, the following orbital ordering (in order of increasing orbital energy) was found to be operative: $d_{xy} < d_{xz} = d_{yz} \leq d_z^2 < d_{x^2-y^2}$. The square-antiprism geometry does not lead to large energy gaps between the d orbitals, which leads to an $S = 2$ ground state for the Fe(II) complex. Nevertheless, the d_{xy} orbital has significantly lower energy relative to that of the d_{xz} and d_{yz} orbitals. Accordingly, the ground state of the Fe(II) complex corresponds unambiguously to a $d_{xy}^2 d_{xz}^1 d_{yz}^1 d_z^2 d_{x^2-y^2}^1$ electronic configuration. Unsurprisingly, the Mn(II) complex has an $S = 5/2$ ground state and no low-energy d-d excited states within 1.0 eV of the ground state. The Co(II) complex, on the other hand, has both a low-lying $S = 1/2$ state and multiple low-energy $S = 3/2$ states. Very long metal–nitrogen bonds are predicted for the Ni(II) and Cu(II) complexes; these bonds may be too fragile to survive in solution or in the solid state, and the complexes may therefore not be isolable. Overall, the different exchange–correlation functionals provided a qualitatively consistent and plausible picture of the low-energy d-d excited states of the complexes.



INTRODUCTION

The creation of novel molecules is one of the central aspirations of inorganic chemistry. The novelty in question may pertain to geometric structure, electronic structure, chemical reactivity, or a combination of these factors. Today, the synthesis of such molecules frequently opens promising avenues of theoretical exploration. Recent syntheses of low-coordinate transition metal complexes have thus led us to uncover a number of unique features in the bonding of such complexes.^{1,2} Recently, we have also contributed to what might be viewed as the opposite end of the spectrum—iron complexes with unusually high coordination numbers.³ As shown in Figure 1(a), Harrop and co-workers, using tetradentate nitrogen ligands referred to hereafter as L_{N4} , synthesized stable eight-coordinate iron(II) complexes.⁴ An alternative perspective shown in Figure 1(b) highlights the D_{2d} square-antiprism stereochemistry of these complexes; each ligand spans two adjacent corners of a square face and then wraps around the metal to occupy two adjacent corners of the other square face of the antiprism. Magnetic susceptibility measurements and Mössbauer spectroscopy

established $S = 2$ ground states for these species, which we were also able to reproduce by preliminary density functional theory (DFT) calculations. Subsequently, Harrop and co-workers also reported analogous eight-coordinate $S = 5/2$ Mn(II) complexes.⁵

Here, we present a DFT study on $[M^{II}(L_{N4})_2]^{2+}$ complexes, where $M = \text{Mn, Fe, Co, Ni, or Cu}$. Our motivations are broadly two-fold: to map out the energetics of the low-lying states of the eight-coordinate complexes, which is a fundamental coordination chemistry question for any novel family of complexes and an especially important one for Fe(II) complexes, many of which have multiple low-energy excited states, and to evaluate DFT performance with regard to both coordination geometry (particularly metal–ligand bond distances) and spin-state energetics. The latter constitutes one of the most difficult problems facing contemporary DFT studies: no exchange–correlation functional provides a universally

Received: September 20, 2014

Published: January 9, 2015

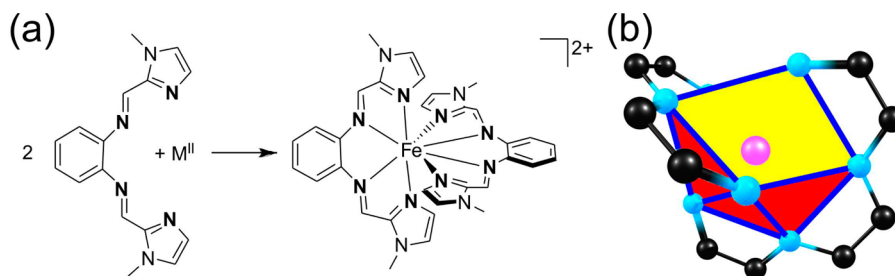


Figure 1. (a) L_{N4} ligand and $[\text{Fe}^{\text{II}}(L_{N4})_2]^{2+}$ complex. (b) L_{N4} skeleton mapped onto a square-antiprism coordination framework.

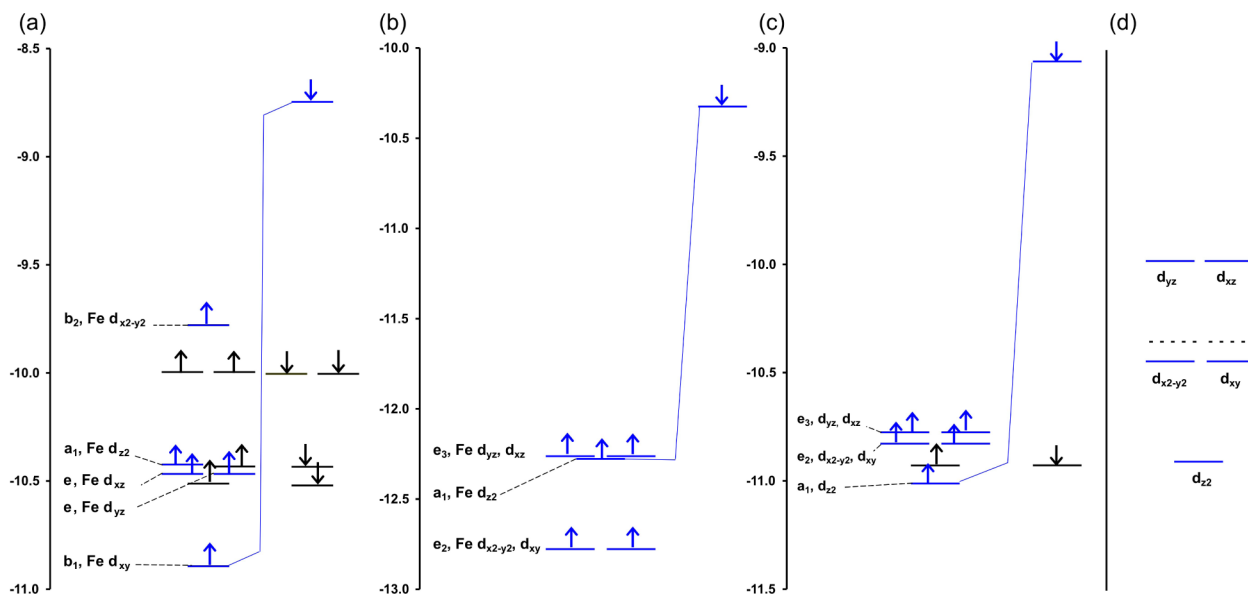


Figure 2. PW91/TZP Kohn–Sham energy levels (eV) for the $S = 2$ ground states of (a) $[\text{Fe}^{\text{II}}(L_{N4})_2]^{2+}$ (D_{2d}), (b) $[\text{Fe}^{\text{II}}(\text{NH}_3)_8]^{2+}$ (D_{4d}), and (c) $[\text{Fe}^{\text{II}}(\text{Py})_8]^{2+}$ (D_{4d}). Electrons in substantially metal-based MOs are indicated in blue; those in primarily ligand-based MOs are shown in black. (d) Crystal field splitting diagrams for a square-antiprism ligand field.

satisfactory description of spin-state energetics for first-row transition metal complexes.⁶ Accordingly, case studies such as the present one can provide valuable guidance for the choice of a suitable functional for DFT studies involving transition metal complexes.

METHODS

All calculations were carried out with the Amsterdam density functional (ADF) program.⁷ In particular, the L_{N4} complexes were all fully optimized under a D_{2d} symmetry constraint.⁸ Various electronic configurations were examined by specifying different electron occupancies for the different irreducible representations. In cases where a D_{2d} symmetry constraint would lead to a degenerate electronic configuration, optimization was carried out under lower symmetry such as D_2 . A suitable grid for numerical integration of matrix elements and tight convergence criteria for both SCF and geometry iterations was employed using the ADF program. Four different functionals, PW91,⁹ BP86,¹⁰ OLYP,^{11,12} and B3LYP^{12,13} (20% Hartree–Fock exchange), were generally used; in addition, Grimme’s dispersion corrections D¹⁴ and D3¹⁵ were applied in conjunction with the BP86 functional. Optimized Cartesian coordinates of key low-energy occupations for each of the functionals are available in the Supporting Information.

RESULTS AND DISCUSSION

(a). Elementary Energy Level Considerations. Figure 2 presents the Kohn–Sham energy levels for several highest-occupied molecular orbitals (HOMOs) for $[\text{Fe}^{\text{II}}(L_{N4})_2]^{2+}$ (D_{2d})

as well as for hypothetical, symmetry-constrained D_{4d} complexes $[\text{Fe}^{\text{II}}(\text{NH}_3)_8]^{2+}$ and $[\text{Fe}^{\text{II}}(\text{Py})_8]^{2+}$ ($\text{Py} = \text{pyridine}$); the diagrams all refer to $S = 2$ ground states of the complexes. Consistent with the unambiguous high-spin ground states, the orbital energies of the d-based frontier molecular orbitals (MOs) all occur within the narrow bandwidth of 0.5–1.0 eV for a given spin symmetry. Note the interesting differences in orbital ordering among the three complexes; these are in part attributable to differences in symmetry (D_{2d} versus D_{4d}) among the complexes.

Figure 3 presents plots of the d-based frontier MOs of the ground state of $[\text{Fe}^{\text{II}}(L_{N4})_2]^{2+}$ (i.e., the energy levels indicated in blue in Figure 2(a)). The plots provide insight into the orbital ordering shown in Figure 2(a). The four imidazole ligands, which are stronger ligands than the imine moieties, define an equatorial square that largely dictates the quantization of d-orbital angular momenta. Thus, among the α -spin (majority-spin) occupied MOs, the MO based on the $d_{x^2-y^2}$ orbital, whose lobes point toward the imidazole nitrogens, has the highest orbital energy. Unsurprisingly, the MO based on the d_{xy} orbital, whose lobes point between the imidazole nitrogens, has the lowest orbital energy, and the β -spin partner of this MO is the overall HOMO for the $S = 2$ d^6 complex. The remaining three Fe-three-dimensional (3D)-based α -spin occupied MOs engage in intermediate levels of metal–ligand antibonding interactions, consistent with intermediate orbital energies that

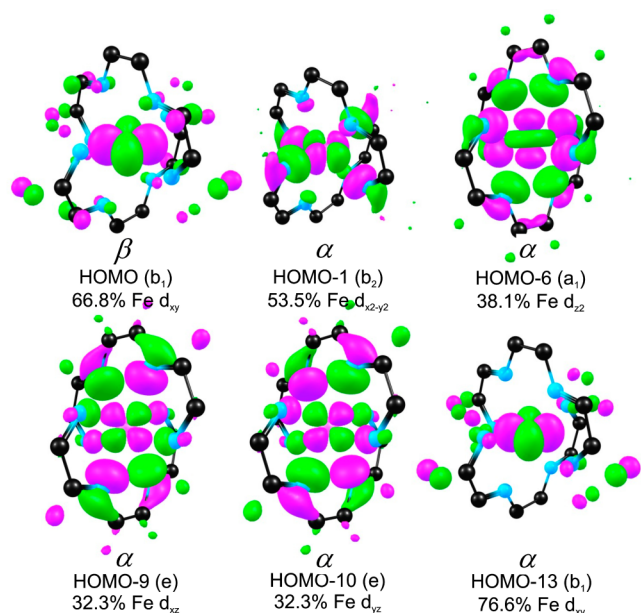


Figure 3. PW91/TZP frontier MOs, with their D_{2d} irreducible representations, for $[\text{Fe}^{\text{II}}(\text{L}_{\text{N}4})_2]^{2+}$ ($S = 2$, contour = $0.04 \text{ e}/\text{\AA}^3$). For clarity, Fe–N bonds and peripheral atoms are not shown.

are roughly halfway between those of the $d_{x^2-y^2}$ and d_{xy} orbitals. The ground-state electronic configuration of the iron complex is thus unambiguously $d_{xy}^2 d_{xz}^1 d_{yz}^1 d_{z^2}^1 d_{x^2-y^2}^1$.

The same orbital energy ordering may also be expected for the other $[\text{M}^{\text{II}}(\text{L}_{\text{N}4})_2]^{2+}$ complexes examined in this study. Thus, for $d^5 \text{Mn}(\text{II})$, which has an inherent tendency for high-spin states, the calculations clearly indicated an $S = 5/2$ ground state and no other low-energy excited states. For $d^7 \text{Co}(\text{II})$, on the other hand, the energy level ordering described above suggests multiple possible low-energy states, which was indeed found to be the case according to our calculations, and is discussed further in section (c).

(b). Molecular Geometries. The two available X-ray structures, $\text{Mn}(\text{II})^5$ and $\text{Fe}(\text{II})^4$ complexes, provide a valuable calibration of the DFT-optimized geometries. Table 1 lists the $\text{M}-\text{N}_{\text{imid}}$ and $\text{M}-\text{N}_{\text{imine}}$ distances that provide the most critical test of the functionals employed, where N_{imid} refers to the coordinating nitrogens of the imidazole units and N_{imine} to those of the imine units. Some of the same information is presented in visual form for $\text{Mn}(\text{II})$ and $\text{Fe}(\text{II})$ in Figures 4 and 5, respectively. Without dispersion corrections, all of the functionals tested—the classical, pure functionals PW91 and BP86; the newer, improved pure functional OLYP based on the OPTX exchange functional; and the hybrid functional B3LYP—overestimate $\text{M}-\text{N}$ distances compared with the experimental values. The differences are smallest for pure functionals PW91 and BP86 (~ 0.03 – 0.04 \AA), somewhat larger for B3LYP (~ 0.05 – 0.08 \AA), and surprisingly largest for OLYP¹⁶ (~ 0.1 – 0.2 \AA for Mn and 0.07 – 0.09 \AA for Fe). Grimme's dispersion corrections D and D3 applied in conjunction with the BP86 functional result in minor improvements in the Mn–N distances but not in the Fe–N distances.

Ten alternative structures, ranging from four- to seven-coordinate, were also examined for the different metal ions studied. These are depicted schematically in Figure 6. For $\text{Mn}(\text{II})$ and $\text{Fe}(\text{II})$, the observed eight-coordinate structures are

Table 1. Optimized $\text{M}-\text{N}$ Distances for Selected Low-Energy States of $[\text{M}^{\text{II}}(\text{L}_{\text{N}4})_2]^{2+}$ Complexes

	S	d^n	d occupations						PW91		OLYP		B3LYP		BP86		BP86-D		BP86-D3	
			d_{xy}	d_{xz}	d_{yz}	d_{z^2}	$d_{x^2-y^2}$	d_{xy}	$\text{M}-\text{N}_{\text{imid}}$	$\text{M}-\text{N}_{\text{imine}}$	$\text{M}-\text{N}_{\text{imid}}$	$\text{M}-\text{N}_{\text{imine}}$	$\text{M}-\text{N}_{\text{imid}}$	$\text{M}-\text{N}_{\text{imine}}$	$\text{M}-\text{N}_{\text{imid}}$	$\text{M}-\text{N}_{\text{imine}}$	$\text{M}-\text{N}_{\text{imid}}$	$\text{M}-\text{N}_{\text{imine}}$	$\text{M}-\text{N}_{\text{imid}}$	$\text{M}-\text{N}_{\text{imine}}$
Mn^{2+}	5/2	5	1	1	1	1	1	1	2.324	2.529	2.324	2.529	2.340	2.566	2.333	2.537	2.266	2.488	2.274	2.538
Fe^{2+}	2	6	2	1	1	1	1	1	2.254	2.434	2.319	2.522	2.297	2.488	2.257	2.446	2.200	2.419	2.208	2.461
Co^{2+}	1/2	7	2	2	2	1	0	1	1.973	2.901	2.009	3.019	2.015	2.923	1.976	2.915	1.958	2.846	1.956	2.893
	3/2	7	2	1	1	2	1	1	2.242	2.487	2.276	2.654	2.242	2.573	2.238	2.513	2.185	2.470	2.189	2.518
	3/2	7	2	1	2	1	1	1	2.175	2.609	2.221	2.757	2.204	2.655	2.179	2.624	2.136	2.560	2.148	2.598
Ni^{2+}	0	8	2	2	2	2	0	0	1.940	2.992	1.980	3.097	1.971	3.008	1.942	3.005	1.924	2.936	1.964	2.975
	1	8	2	2	2	1	1	1	2.114	2.733	2.154	2.891	2.140	2.750	2.116	2.752	2.082	2.672	2.090	2.713
	1	8	2	1	1	2	2	2	2.920	2.028	3.105	2.067	2.841	2.079	2.961	2.028	2.825	2.028	2.811	2.034
Cu^{2+}	1/2	9	2	2	2	2	1	1	2.069	2.867	2.114	3.048	2.085	2.876	2.072	2.886	2.044	2.779	2.047	2.832

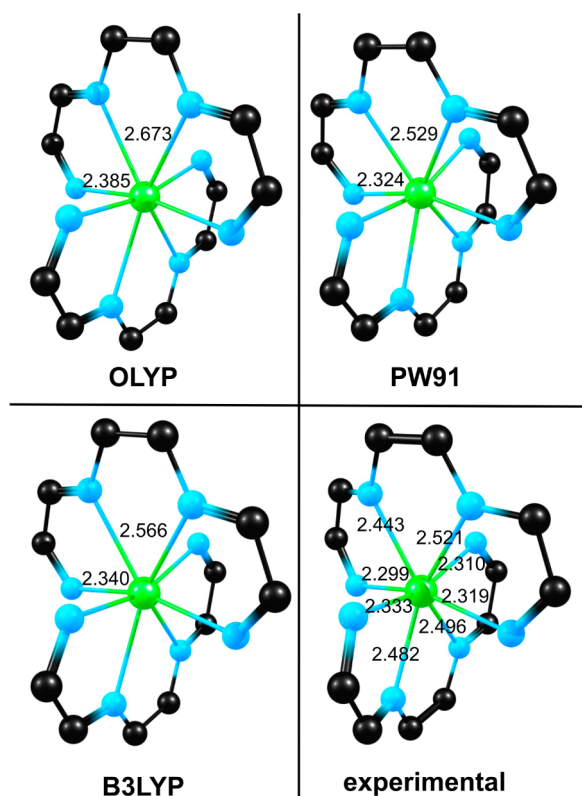


Figure 4. Experimental and optimized Mn–N distances for $[\text{Mn}^{\text{II}}(\text{L}_{\text{N}4})_2]^{2+}$. Peripheral atoms have been omitted for clarity.

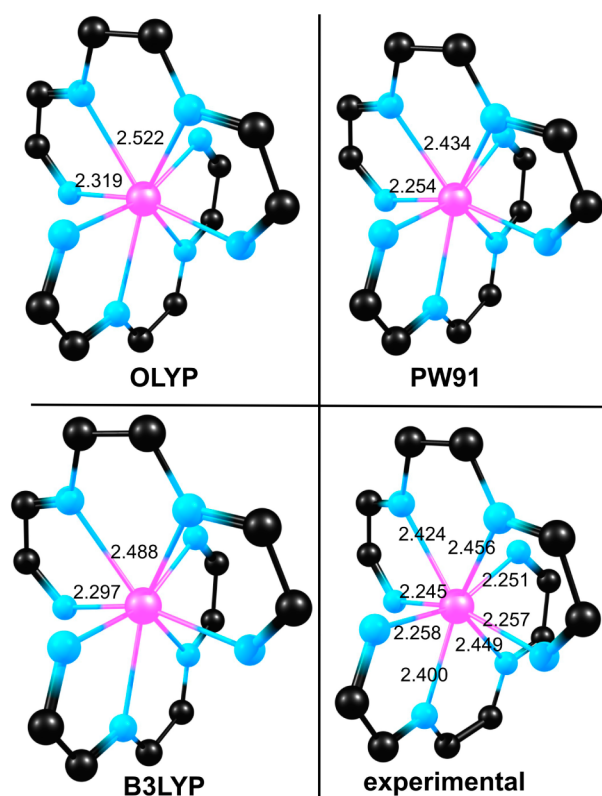


Figure 5. Experimental and optimized Fe–N distances for $[\text{Fe}^{\text{II}}(\text{L}_{\text{N}4})_2]^{2+}$. Peripheral atoms have been omitted for clarity.

found to be global minima, a conclusion that appears to be supported by significant precedence in the literature; there are

many examples of eight-coordinate Mn^{17} and Fe complexes^{18,19} with suitable polydentate ligands. For eight-coordinate Co, Ni, and Cu, on the other hand, the $\text{M}-\text{N}_{\text{imine}}$ bonds are generally predicted to be quite long (2.5–3.0 Å), which questions the stability of these complexes. In fact, for both $\text{Co}(\text{II})$ and $\text{Cu}(\text{II})$, the lowest-energy associations with $\text{L}_{\text{N}4}$ appear to be five-coordinate and $S = 1/2$, whereas for $\text{Ni}(\text{II})$ the lowest-energy state appears to be six-coordinate and $S = 1$. In each of these cases (Co, Ni, and Cu), the eight-coordinate form is ~ 0.2 – 0.4 eV higher in energy relative to the global minimum.

(c). Spin-State Energetics. Table 2 presents relative energies for selected low-energy states for the eight-coordinate complexes $[\text{M}^{\text{II}}(\text{L}_{\text{N}4})_2]^{2+}$, where $\text{M} = \text{Fe}, \text{Co}, \text{Ni},$ or Cu . The data are derived from full geometry optimizations under appropriate symmetry constraints for a wide range of specified occupations that correspond to low-energy electronic states of interest. To our knowledge, these results provide the first reasonably detailed picture of the excited-state architecture of eight-coordinate square-antiprismatic transition metal complexes. The primary findings for the different metal complexes are as follows.

Mn(II). As mentioned above, the d^5 $\text{Mn}(\text{II})$ complex has the expected $S = 5/2$ ground state⁵ and no d–d excited states within 1.0 eV of that state. The electronic-state architecture of the $\text{Mn}(\text{II})$ complex is thus not of great interest as far as this study is concerned, especially given manganese's inherent preference for high-spin states. It is worth noting however that an $S = 5/2$ ground state has also been observed for the isoelectronic $[\text{Fe}^{\text{III}}(\text{L}_{\text{N}4})_2]^{3+}$ complex.⁴

Fe(II). The d^6 $\text{Fe}(\text{II})$ case is far more interesting, and the calculated energetics provide deep insight into the orbital structure of this class of square-antiprismatic complexes. All the functionals examined unambiguously indicate an $S = 2$ ground state with a $d_{xy}^2 d_{xz}^1 d_{yz}^1 d_{z^2}^1 d_{x^2-y^2}^1$ orbital occupancy. The next higher state, which is actually a degenerate pair ~ 0.5 eV higher (the exact value depends on the functional), involves excitation of an electron from the d_{xy} to the d_{xz} or the d_{yz} orbital. Next are the $d_{z^2}^2$ and $d_{x^2-y^2}^2$ configurations, which are roughly 1 eV above the ground state (the exact energy value is again somewhat dependent on the functional).

Co(II). The cobalt complex, which has not yet been reported, is of interest as a possible spin-crossover system. According to the data presented in Table 2, two different states ($S = 1/2$ and $3/2$) are equally plausible contenders for the ground state; for all of the functionals examined, the two states differ by no more than 0.21 eV in energy. They may be described by the following electronic configurations:

$$S = 1/2: d_{xy}^2 d_{xz}^2 d_{yz}^2 d_{z^2}^1 d_{x^2-y^2}^0$$

$$S = 3/2: d_{xy}^2 d_{xz}^1 d_{yz}^2 d_{z^2}^1 d_{x^2-y^2}^1$$

Thus, for $\text{Co}(\text{II})$, the energetic cost of populating the $d_{x^2-y^2}^2$ orbital is about the same as the pairing energy for the d_{xz} and d_{yz} orbitals.

Unsurprisingly, in light of these results, two additional low-energy $S = 3/2$ states are predicted at ~ 0.4 eV relative to the ground state. They may be described by the following electronic configurations:

$$S = 3/2: d_{xy}^2 d_{xz}^1 d_{yz}^1 d_{z^2}^2 d_{x^2-y^2}^1$$

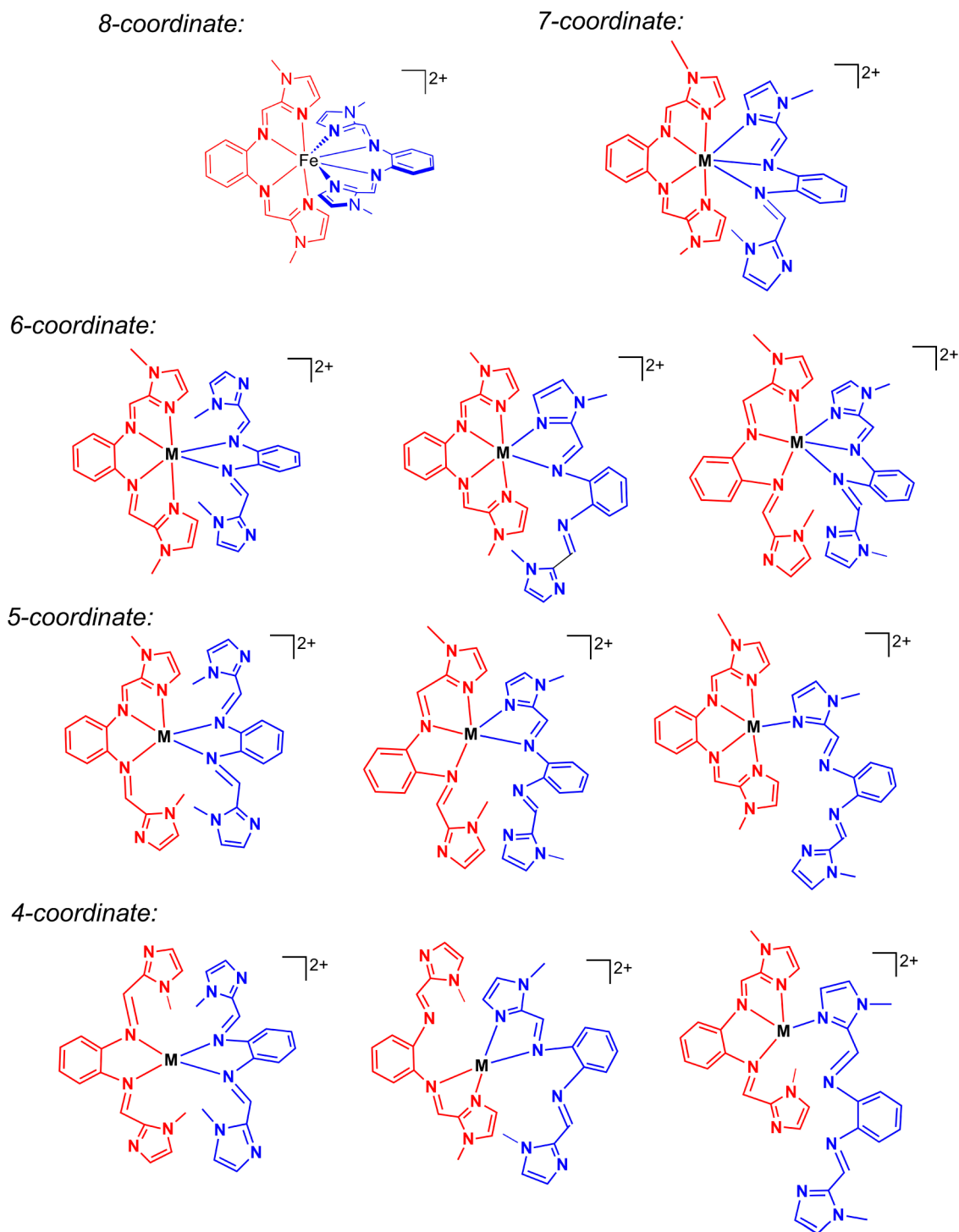


Figure 6. Alternative geometries examined for the various complexes studied.

$$S = 3/2: d_{xy}^1 d_{xz}^2 d_{yz}^2 d_z^1 d_{x^2-y^2}^1$$

Interestingly, the $S = 3/2$ state with the $d_{xy}^2 d_{xz}^1 d_{yz}^1 d_z^1 d_{x^2-y^2}^2$ configuration is also not very high in energy, typically well under 1.0 eV above the ground state for most of the functionals examined.

Of interest is whether the eight-coordinate Co(II) complex might actually exist as a stable entity and be amenable to synthesis and structural characterization. We have already stated above that other stereochemistries with lower coordination numbers appear to be favored for L_{N4} , although only by

~ 0.2 eV. For the lowest-energy $S = 1/2$ state of the eight-coordinate form, the data in Table 1 predict rather long M–N_{imine} distances of 2.9–3.0 Å, which appear to be a consequence of double occupancy of the d_{xz} or d_{yz} orbitals. These long bonds may be too fragile to persist in solution or in the solid state. Significantly shorter M–N_{imine} distances of about 2.5 Å, however, are predicted for the lowest $S = 3/2$ state of the complex. The calculated Co–N bond distances for the lowest $S = 3/2$ state of $[\text{Co}^{\text{II}}(\text{L}_{N4})_2]^{2+}$ are actually not very different from those observed for an $S = 3/2$ eight-coordinate Co(II) complex with a pair of tetrazamacrocyclic 2,11-diaza-

Table 2. Relative Energies (eV) for Different Electronic Configurations

S	d occupations					relative energy					symm.	occupation			
	d_{xy}	d_{xz}	d_{yz}	d_z	$d_{x^2-y^2}$	PW91	OLYP	B3LYP	BP86	BP86-D	BP86-D3	A1	A2	B1	B2
Fe^{2+}	2	2	1	1	1	0.00	0.00	0.00	0.00	0.00	0.00	D_{2d}	24//23	6//6	24//23
	1	1	1	2	1	1.02	0.79	0.56	0.99	1.16	1.06	D_{2d}	24//24	6//6	24//23
	1	1	1	1	2	1.03	0.68	0.73	0.98	1.32	1.25	D_{2d}	24//23	6//6	24//24
	1	1	2	1	1	0.61	0.41	0.23	0.59	0.76	0.65	A	B1	B2	B3
Co^{2+}	1/2	2	2	2	1	0.00	0.20	0.36	0.00	0.00	0.00	D_{2d}	31//29	30//29	29//28
	1	2	2	2	0	1.87	1.98	2.33	1.85	1.93	1.88	D_{2d}	24//23	6//6	23//23
	2	2	2	0	1	3.82	3.90	5.53	3.81	3.97	3.87	D_{2d}	24//24	6//6	23//22
	2	1	2	2	0	0.83	0.99	1.19	0.83	0.84	0.83	A	B1	B2	B3
Co^{2+}	3/2	2	1	1	2	0.37	0.24	0.21	0.36	0.34	0.43	D_{2d}	31//31	29//29	29//28
	1	1	1	2	2	0.65	0.27	0.56	0.59	0.95	1.01	D_{2d}	24//24	6//6	24//23
	2	1	1	1	2	1.25	0.91	1.49	1.23	1.38	1.46	D_{2d}	24//23	6//6	24//24
	1	2	2	1	1	0.49	0.20	0.22	0.46	0.59	0.59	D_{2d}	24//23	6//6	24//23
Ni^{2+}	0	2	2	2	0	0.07	0.28	0.61	0.07	0.06	0.05	A	B1	B2	B3
	1	2	2	1	1	0.00	0.00	0.00	0.00	0.00	0.00	D_{2d}	31//30	30//29	29//28
	1	2	2	2	1	1.32	1.10	1.37	1.30	1.41	1.35	D_{2d}	31//29	30//30	29//28
	1	2	2	1	2	1.34	1.15	1.12	1.33	1.46	1.43	A	A2	B1	B2
Cu^{2+}	2	1	2	2	1	0.61	0.56	0.63	0.61	0.59	0.60	D_{2d}	24//24	6//6	23//23
	1	1	2	2	2	0.90	0.68	1.00	0.86	1.12	1.14	D_{2d}	24//23	6//6	24//23
	2	2	2	1	2	0.37	0.18	0.70	0.33	0.63	0.66	D_{2d}	24//24	6//6	24//24
	2	2	2	2	2	0.61	0.56	0.63	0.61	0.59	0.60	A	B1	B2	B3
Cu^{2+}	1/2	2	2	2	1	0.00	0.00	0.00	0.00	0.00	0.00	D_{2d}	31//31	30//29	29//28
	1	2	2	2	2	1.43	1.07	1.45	1.41	1.57	1.54	D_{2d}	31//30	30//30	29//28
	2	2	2	1	2	0.88	0.78	0.97	0.89	0.91	0.95	A	A2	B1	B2
	2	1	2	2	2	0.97	0.79	0.66	0.97	1.04	1.07	A	A1	B1	B2

[3.3](2,6)pyridinophane ligands, where the average Co-N_{py} and Co-N_{amine} distances are 2.31 and 2.39 Å, respectively.²⁰ Synthesis of an eight-coordinate Co(II) complex with an L_{N4}-type ligand is thus an intriguing future goal.^{21,22}

Ni(II). As in the case of Co(II), two different electronic configurations appear to be equally plausible contenders for the ground state for a potential eight-coordinate complex:

$$S = 1: d_{xy}^2 d_{xz}^2 d_{yz}^2 d_{z^2}^1 d_{x^2-y^2}^1$$

$$S = 0: d_{xy}^2 d_{xz}^2 d_{yz}^2 d_{z^2}^2 d_{x^2-y^2}^0$$

Most of the functionals predict the triplet state above to be of lowest energy, with the singlet state only ~0.1 eV higher in energy. The other d-d excited triplet occurs a few to several tenths of an eV above these two lowest states.

Cu(II). For Cu(II), the $S = 1/2$ ground state is unambiguously $d_{xy}^2 d_{xz}^2 d_{yz}^2 d_{z^2}^2 d_{x^2-y^2}^1$. The lowest d-d excited state is well over half an eV above the ground state.

As mentioned above, our calculations predict rather long M-N_{imine} distances of 2.7–2.9 Å for both Ni(II) and Cu(II). Unless special ligands can be developed that protect such fragile bonds (e.g., via encapsulation), eight-coordinate Ni²³ and Cu²⁴ complexes appear likely to remain elusive.

(d). Spin Density Profiles. Figure 7 depicts calculated PW91/TZP spin density profiles for the lowest-energy open-shell states of the various complexes studied. Table 3 lists selected Mulliken spin populations for three different functionals. The spin density profiles are not of particular interest by themselves; however, a few comments are warranted in the interest of having a more complete description of the results. The fact that the spin populations are exceedingly similar for the various functionals is reassuring, indicating that the different functionals afford very similar descriptions of metal–ligand bonding. In each case, the spin density is highly localized on the metal center, with the localization being greatest for Mn(II). The relative magnitude of N_{imid}/N_{imine} spin populations may be qualitatively rationalized in terms of the orbital occupancies. Thus, single occupancy of the $d_{x^2-y^2}$ orbital results in small but significant N_{imid} spin populations, whereas significant N_{imine} spin populations are generally attributable to singly occupied d_{xz} / d_{yz} orbitals. None of the calculated spin density profiles, including those not depicted in Figure 7, evince any significant traces of negative or minority spin density, indicating that the L_{N4} ligands are essentially “innocent”.

CONCLUSIONS

The first detailed DFT study has been carried out on eight-coordinate square-antiprismatic first-row transition metal complexes, involving Mn(II), Fe(II), Co(II), Ni(II), and Cu(II), along with a pair of tetradentate N₄ ligands. Of these, the Mn(II) and Fe(II) complexes have been synthesized and characterized structurally,^{4,5} providing valuable calibration for the overall theoretical study. The key motivation has been to obtain an idea of the d-d excited-state architecture within ~1.0 eV of the ground state. This has been achieved reasonably well, and some of the main conclusions are as follows.

1. The various functionals examined, especially PW91, BP86, and B3LYP, all provide reasonably good optimized structures as judged by comparison with the two crystallographic structures. As commonly observed, all of the functionals overestimate the metal-ligand bond distances slightly; somewhat surprisingly, this discrepancy is the worst for OLYP, a pure functional that

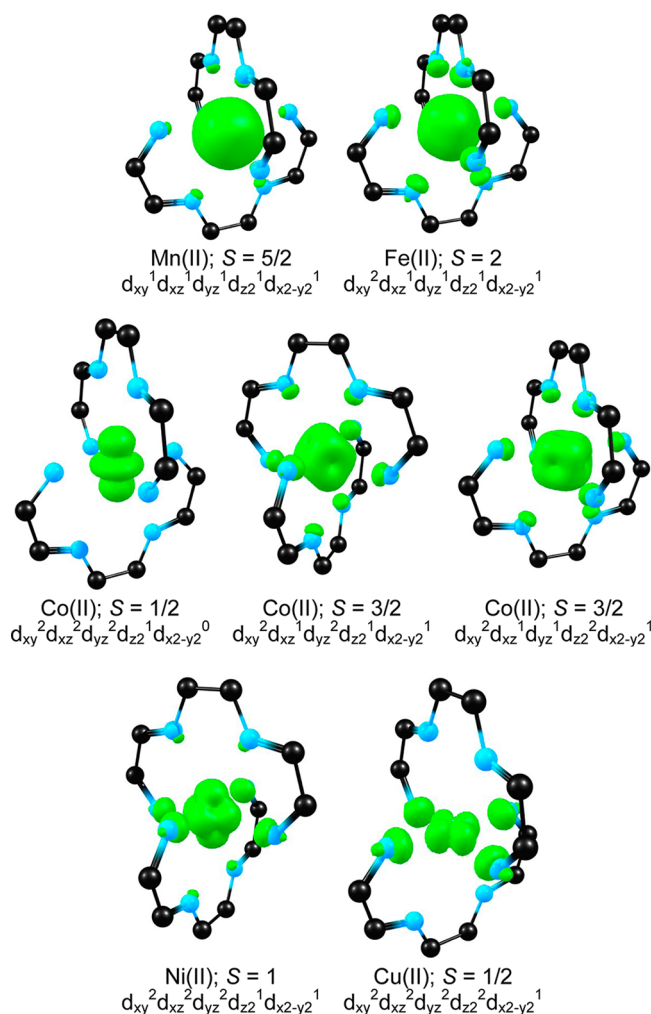


Figure 7. PW91/TZP spin density profiles for the lowest-energy open-shell states of $[M^{II}(L_{N4})_2]^{2+}$ complexes. The isodensity contour value used is 0.09 e/Å³.

we generally found to be one of the best in our earlier work. Dispersion corrections applied to the BP86 functional led to shorter, improved distances, but these still fell short of truly excellent agreement with the experimental results.

2. The imidazole groups in the L_{N4} molecule are stronger ligands than the amine groups and dictate the spatial disposition of the d orbitals. The four coordinating nitrogens from the imidazole group may be thought of as defining a square in the *xy* plane, with two imine nitrogens above and two below. Understandably, the $d_{x^2-y^2}$ orbital, whose lobes point toward the imidazole nitrogens, has the highest orbital energy among the five d orbitals. In general, the following orbital ordering (in order of increasing orbital energy) was found to hold for all of the complexes:

$$d_{xy} < d_{xz} = d_{yz} \leq d_{z^2} < d_{x^2-y^2}$$

3. The excited-state structure of the Fe(II) complex is of considerable interest. Whereas the square-antiprism geometry does not lead to large energy gaps between the d orbitals, which accounts for the $S = 2$ ground state, the d_{xy} orbital still has energy that is significantly lower than that of the d_{xz} or d_{yz} orbitals. The ground state thus corresponds unambiguously to a $d_{xy}^2 d_{xz}^1 d_{yz}^1 d_{z^2}^1 d_{x^2-y^2}^1$ electronic configuration.

Table 3. Mulliken Spin Populations for $[M^{II}(L_{N4})_2]^{2+}$

	S	d occupations						PW91			OLYP			B3LYP		
		d^z	d_{xy}	d_{xz}	d_{yz}	d_z^2	$d_{x^2-y^2}$	M	N_{imid}	N_{imine}	M	N_{imid}	N_{imine}	M	N_{imid}	N_{imine}
Mn ²⁺	5/2	5	1	1	1	1	1	4.820	0.004	0.012	4.865	0.007	0.010	4.821	0.013	0.016
Fe ²⁺	2	6	2	1	1	1	1	3.775	0.046	0.049	3.759	0.046	0.045	3.773	0.037	0.030
Co ²⁺	1/2	7	2	2	2	1	0	1.042	−0.009	0.007	1.047	−0.008	0.004	1.027	−0.007	0.004
	3/2	7	2	1	1	2	1	2.678	0.043	0.036	2.692	0.044	0.030	2.790	0.034	0.017
	3/2	7	2	1	2	1	1	2.656	0.051	0.033	2.658	0.054	0.028	2.767	0.041	0.016
Ni ²⁺	0	8	2	2	2	2	0	0.000	0.000	0.000	0.000	0.000	0.000	0.000	0.000	0.000
	1	8	2	2	2	1	1	1.585	0.073	0.023	1.562	0.080	0.021	1.716	0.059	0.010
	1	8	2	1	1	2	2	1.509	0.014	0.071	1.518	0.007	0.074	1.678	0.008	0.058
Cu ²⁺	1/2	9	2	2	2	2	1	0.567	0.098	−0.001	0.546	0.103	−0.001	0.647	0.084	−0.002

4. For Co(II), an $S = 1/2$ state and an $S = 3/2$ state appear to compete for the ground state, with multiple additional $S = 3/2$ states a few tenths of an eV higher in energy. Rather long Co- N_{imine} distances (2.9–3.0 Å) are predicted for a number of these states; these long bonds may well be too fragile to exist in the condensed phase. The lowest $S = 3/2$ state, with Co- N_{imine} distances of about 2.5 Å, appears to be the most promising candidate for synthesis and structural characterization.

5. Long and therefore presumably fragile M- N_{imine} bonds are also predicted for the eight-coordinate Ni(II) and Cu(II) complexes. Their experimental accessibility is thus questionable.

6. The various functionals examined provide a qualitatively consistent picture of the excited-state energetics of the complexes. As is well-known, this is often not the case for transition metal complexes, especially for energy differences involving high- versus low-spin states of Fe(II) and Fe(III) complexes. A plausible reason is that we have largely compared calculations in which ΔM_S is either 0 or ± 1 , whereas the notoriously poor Fe calculations typically involve $\Delta M_S = \pm 2$.²⁵

■ ASSOCIATED CONTENT

Supporting Information

Optimized Cartesian coordinates of key low-energy occupations for each of the functionals. This material is available free of charge via the Internet at <http://pubs.acs.org>.

■ AUTHOR INFORMATION

Corresponding Author

*E-mail: abhik@chem.uit.no.

Notes

The authors declare no competing financial interest.

■ ACKNOWLEDGMENTS

This work was supported by the Research Council of Norway (A.G.), the South African National Research Foundation and the Central Research Fund of the University of the Free State in Bloemfontein (J.C.), and the University of Georgia Research Foundation (T.C.H.).

■ REFERENCES

- (1) (a) Review: Mehn, M. P.; Peters, J. C. *J. Inorg. Biochem.* **2006**, *100*, 634–643. (b) Dai, X. L.; Kapoor, P.; Warren, T. H. *J. Am. Chem. Soc.* **2004**, *126*, 4798–4799. (c) Review: Holland, P. L. *Acc. Chem. Res.* **2008**, *41*, 905–914.
- (2) Theoretical studies on low-coordinate complexes: (a) Tangen, E.; Conradie, J.; Ghosh, A. *J. Chem. Theory Comput.* **2007**, *3*, 448–457. (b) Conradie, J.; Ghosh, A. *J. Chem. Theory Comput.* **2007**, *3*, 689–702. (c) Wasbotten, I. H.; Ghosh, A. *Inorg. Chem.* **2007**, *46*, 7890–

7898. (d) Aquilante, F.; Malmqvist, P.-Å.; Pedersen, T. B.; Ghosh, A.; Roos, B. O. *J. Chem. Theory Comput.* **2008**, *4*, 694–702. (e) Conradie, J.; Ghosh, A. *J. Chem. Theory Comput.* **2008**, *4*, 1576–1584. (f) Conradie, J.; Ghosh, A. *Inorg. Chem.* **2010**, *49*, 243–248.

- (3) (a) Lippard, S. J. *Prog. Inorg. Chem.* **1967**, *8*, 109–193. (b) Wang, S.; Westmoreland, T. D. *Inorg. Chem.* **2009**, *48*, 719. (c) Muetterties, E. L. *Inorg. Chem.* **1973**, *12*, 1963.

- (4) Patra, A. K.; Dube, K. S.; Papaefthymiou, G. C.; Conradie, J.; Ghosh, A.; Harrop, T. C. *Inorg. Chem.* **2010**, *49*, 2032–2034.

- (5) Dube, K. S.; Harrop, T. C. *Dalton Trans.* **2011**, *40*, 7496–7498.

- (6) The original literature on this topic spans $\sim 10^3$ papers at this time; fortunately, this area has been reviewed periodically: (a) Ghosh, A.; Taylor, P. R. *Curr. Opin. Chem. Biol.* **2003**, *7*, 113–124. (b) Harvey, J. N. *Struct. Bonding (Berlin, Ger.)* **2004**, *112*, 151–183. (c) Ghosh, A. *J. Biol. Inorg. Chem.* **2006**, *11*, 712–724. (d) Neese, F.; Liakos, D. G.; Ye, S. J. *Biol. Inorg. Chem.* **2011**, *16*, 821–829. (e) Swart, M. *Int. J. Quantum Chem.* **2013**, *113*, 2–7.

- (7) *Amsterdam Density Functional Program*; Division of Theoretical Chemistry, Vrije Universiteit: De Boelelaan 1083, 1081 HV Amsterdam, The Netherlands. www.scm.com.

- (8) As described below, a wide variety of alternative geometries and coordination numbers were also examined with symmetry-unconstrained geometry optimizations.

- (9) Perdew, J. P.; Chevary, J. A.; Vosko, S. H.; Jackson, K. A.; Pederson, M. R.; Singh, D. J.; Fiolhais, C. *Phys. Rev. B* **1992**, *46*, 6671–6687. Erratum: Perdew, J. P.; Chevary, J. A.; Vosko, S. H.; Jackson, K. A.; Pederson, M. R.; Singh, D. J.; Fiolhais, C. *Phys. Rev. B* **1993**, *48*, 4978.

- (10) (a) Becke, A. D. *Phys. Rev. A* **1988**, *38*, 3098–3100. (b) Perdew, J. P. *Phys. Rev. B* **1986**, *33*, 8822–8824. Erratum: Perdew, J. P. *Phys. Rev. B* **1986**, *34*, 7406.

- (11) The OPTX exchange functional: Handy, N. C.; Cohen, A. J. *Mol. Phys.* **2001**, *99*, 403–412.

- (12) The LYP correlation functional: Lee, C.; Yang, W.; Parr, R. G. *Phys. Rev. B* **1988**, *37*, 785–789.

- (13) Stephens, J.; Devlin, F. J.; Chabalowski, C. F.; Frisch, M. J. *J. Phys. Chem.* **1994**, *98*, 11623–11627.

- (14) Grimme, S. *J. Comput. Chem.* **2006**, *27*, 1787–1799.

- (15) Grimme, S.; Anthony, J.; Ehrlich, S.; Krieg, H. *J. Chem. Phys.* **2010**, *132*, No. 154104.

- (16) It is worth noting that in our experience⁶ OLYP normally served as one of the best functionals for transition metals, specifically vis-à-vis the problem of spin-state energetics. See also: (a) Baker, J.; Pulay, P. *J. Comput. Chem.* **2003**, *24*, 1184–1191. (b) Conradie, J.; Ghosh, A. *J. Phys. Chem. B* **2007**, *111*, 12621–12624. (c) Conradie, M. M.; Conradie, J.; Ghosh, A. *J. Inorg. Biochem.* **2011**, *105*, 84–91.

- (17) A large number of eight-coordinate Mn(II) complexes are known; the following are references to $Mn^{II}N_8$ structures: (a) Park, W.; Cho, J.-H.; Lee, H.-I.; Park, M.; Lah, M. S.; Lim, D. *Polyhedron* **2008**, *27*, 2043–2048. (b) Bu, X.-H.; Chen, W.; Mu, L.-J.; Zhang, Z.-H.; Zhang, R.-H.; Clifford, T. *Polyhedron* **2000**, *19*, 2095–2100. (c) Keypour, H.; Goudarzi, H.; Brisdon, A. K.; Pritchard, R. G.; Rezaei, M. *Inorg. Chim. Acta* **2008**, *361*, 1415–1420. (d) Vaira, M. D.; Mani, F.; Stoppioni, P. *J. Chem. Soc., Dalton Trans.* **1992**, 1127–

1130. (e) Dang, D.; Bai, Y.; Duan, C. *J. Chem. Crystallogr.* **2008**, *38*, 557–560. (f) Gultneh, Y.; Farooq, A.; Karlin, K. D.; Liu, S.; Zubiet, J. *Inorg. Chim. Acta* **1993**, *211*, 171–175. (g) Kim, M.-Y.; Chi, Y.-S.; Han, J.-H. *Bull. Korean Chem. Soc.* **2010**, *31*, 23–24.

(18) Eight-coordinate FeN_8 complexes: (a) Bu, X.-H.; Lu, S.-L.; Zhang, R.-H.; Liu, H.; Zhu, H.-P.; Liu, Q.-T. *Polyhedron* **2000**, *19*, 431–435. (b) Singh, P.; Clearfield, A.; Bernal, I. J. *Coord. Chem.* **1971**, *1*, 29–37. (c) Diebold, A.; Hagen, K. S. *Inorg. Chem.* **1998**, *37*, 215–223. (d) Vaira, M. D.; Mani, F.; Stoppioni, P. *J. Chem. Soc., Dalton Trans.* **1992**, 1127–1130. (e) Koch, W. O.; Barbieri, A.; Grodzicki, M.; Schunemann, V.; Trautwein, A. X.; Krüger, H.-J. *Angew. Chem., Int. Ed.* **1996**, *35*, 422–424.

(19) Eight-coordinate FeO_8 complexes: (a) Meier, K.; Rihs, G. *Angew. Chem., Int. Ed. Engl.* **1985**, *24*, 858–862. (b) Fiolka, C.; Pantenburg, I.; Meyer, G. *Cryst. Growth Des.* **2011**, *11*, 5159–5165.

(20) Koch, W. O.; Kaiser, J. T.; Krüger, H.-J. *Chem. Commun. (Cambridge, U.K.)* **1997**, 2237–2238.

(21) Eight-coordinate $\text{Co}^{\text{II}}\text{N}_8$ structures: (a) Koch, W. O.; Kaiser, J. T.; Krüger, H.-J. *Chem. Commun. (Cambridge, U.K.)* **1997**, 2237–2238. (b) Wang, W.-Z.; Wu, Y.; Ismayilov, R. H.; Kuo, J.-H.; Yeh, C.-Y.; Lee, H.-W.; Fu, M.-D.; Chen, C.-H.; Lee, G.-H.; Peng, S.-M. *J. Chem. Soc., Dalton Trans.* **2014**, *43*, 6229–6231.

(22) Eight-coordinate $\text{Co}^{\text{II}}\text{O}_8$ structures: (a) Fiolka, C.; Pantenburg, I.; Meyer, G. *Cryst. Growth Des.* **2011**, *11*, 5159–5165. (b) Duan, X.; Guo, L.; Wang, J. *Huaxue Xuebao* **2013**, *71*, 107–113.

(23) Eight-coordinate Ni: Fiolka, C.; Pantenburg, I.; Meyer, G. *Cryst. Growth Des.* **2011**, *11*, 5159–5165.

(24) Eight-coordinate Cu: (a) Roberts, S. A.; Bloomquist, D. R.; Willett, R. D.; Dodgen, H. W. *J. Am. Chem. Soc.* **1981**, *103*, 2603–2610. (b) Cingi, M. B.; Lanfredi, A. M. M.; Tiripicchio, A.; Camellini, M. T. *Acta Crystallogr.* **1978**, *B34*, 412–416. (c) Barszcz, B.; Glowiak, T.; Jezierska, J. *Polyhedron* **1999**, *18*, 3713–3721. (d) Wei, M.-L.; Li, H.-H.; Wang, X.-X.; Wang, J.-H. *Struct. Chem.* **2012**, *23*, 129–136. (e) Chen, X.-M.; Mak, T. C. W. *Polyhedron* **1991**, *10*, 273–276.

(25) Another instructive example in which good state energetics seems to parallel a small change in M_S involves the site of reduction for metal versus macrocycle of nickel hydroporphyrins: Ryeng, H.; Gonzalez, E.; Ghosh, A. *J. Phys. Chem. B* **2008**, *112*, 15158–15173.